

Monitoring Low Frequency Propagation with a Software Defined Radio Receiver

Part II ~ Observations

Whitham D. Reeve

II.1. Introduction

Part I of this paper reviews the characteristics of low frequency propagation and how monitoring low frequency communications signals may be used to indirectly observe solar flares through sudden ionospheric disturbances (SID) detection [ReeveP1]. Part II discusses the receiver instrumentation and transmitter characteristics and shows examples of signals received at Cohoe Radio Observatory (CRO) from around the world. No SIDs were observed during the measurement period in September and October 2018, not surprising given the low point in the current solar cycle and lack of significant solar flares, but the instrumentation and methods described here may be applied to monitoring activity in the next solar cycle.

The measurements described here took advantage of experience I gained during the initial installation of the loop antenna and SDR receiver at CRO in June 2018, described in {[Reeve18-1](#)}, and work associated with weak signal reception of the Swedish station SAQ in July 2018, described in ([Reeve18-2](#)).

II.2. Receiver Site Instrumentation

The Cohoe Radio Observatory low frequency receiver station is located in southcentral Alaska on the Kenai Peninsula (figure II.1). The system consists of a shop-built, untuned, 1.2 m diagonal square loop antenna, antenna rotator, SDRPlay RSP2Pro SDR receiver and associated SDRUno software, balanced twisted pair transmission line and Lenovo M910 SFF PC with Windows 10 x64 operating system (figures II.2, II.3, II.4 and II.5). A detailed description of the loop antenna installation at CRO may be found at {[Reeve18-3](#)}.

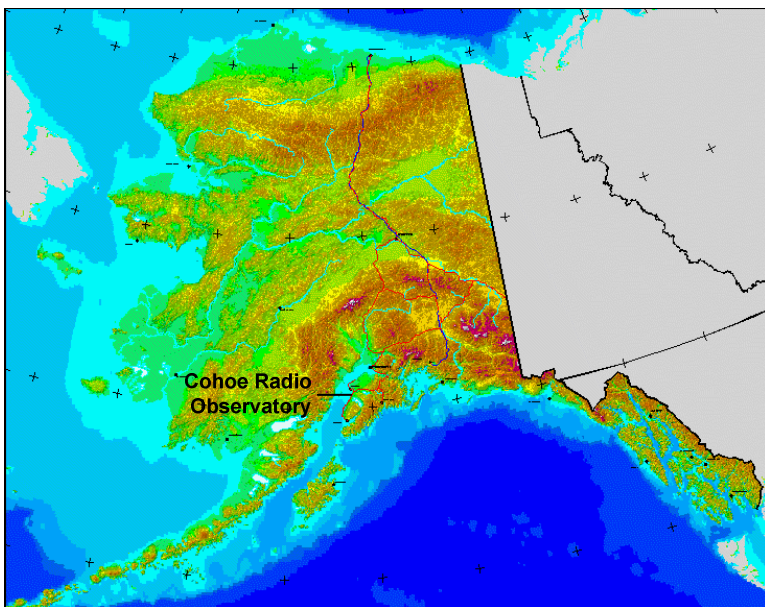


Figure II.1 ~ Partial Alaska map showing location of Cohoe Radio Observatory. The station is in a rural area on the Kenai Peninsula about 120 km southwest of Anchorage. Image source: USGS

Coordinates:

Latitude: 60° 22' 04.7"N

Longitude: 151° 18' 55.1"W

Elevation: 22 m AMSL

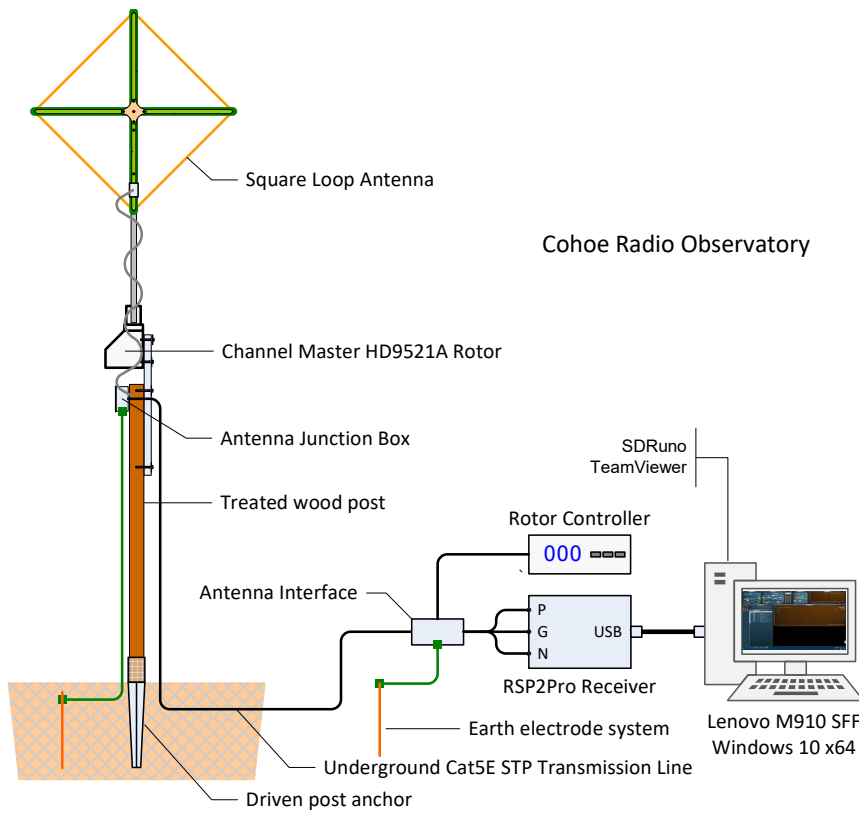


Figure II.2 ~ VLF receiver and antenna system at Cohoe Radio Observatory. The shielded twisted pair Cat5E transmission line is installed in liquid-tight flexible non-metallic conduit and buried just below the ground surface. The antenna is connected to the receiver's 1000 ohm *H/I* Z balanced input through an interface that includes grounded 100 kohm resistors to control common mode currents. The antenna is connected to 1 pair of the STP cable and the rotator is connected to the remaining 3 pairs.

Antenna height: 11.0 ft (3.4 m) AGL

Image © 2018 W. Reeve

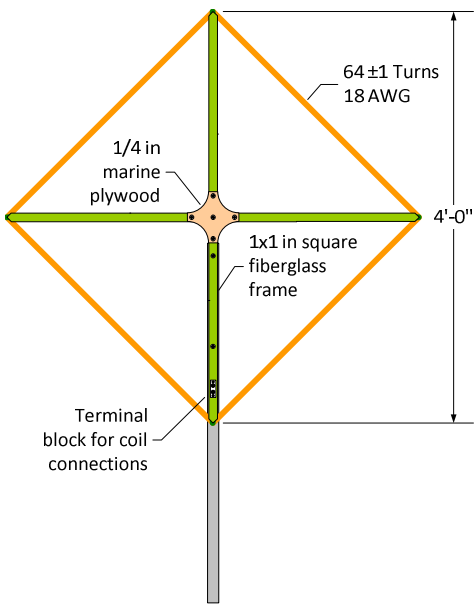


Figure II.3 ~ Shop-built small loop antenna used with the low frequency receiver. The antenna shown here was built in Anchorage in 2009 and stored until it was installed at Cohoe Radio Observatory in mid-2018.

Dimensions:

- Loop diagonal: 4 ft (1.2 m)
- Loop area: 7.9 ft² (0.733 m²)
- Windings: 64 ± 1 turns coated copper magnet wire
- Estimated length of wire: 720± ft (220± m)
- Inductance: 12.27 mH at 1 kHz
- Effective electrical height: 27 mm at 24 kHz
- Tuning: None



Figure II.4 ~ SDRPlay RSP2Pro software defined radio receiver. Dimensions are 99 x 87 x 33 mm, 0.3 kg. The balanced high-impedance antenna interface is the green pluggable connector on far-left. The receiver is powered through its USB connection and draws about 170 mA at 5 Vdc. Images source: SDRPlay, used with permission.

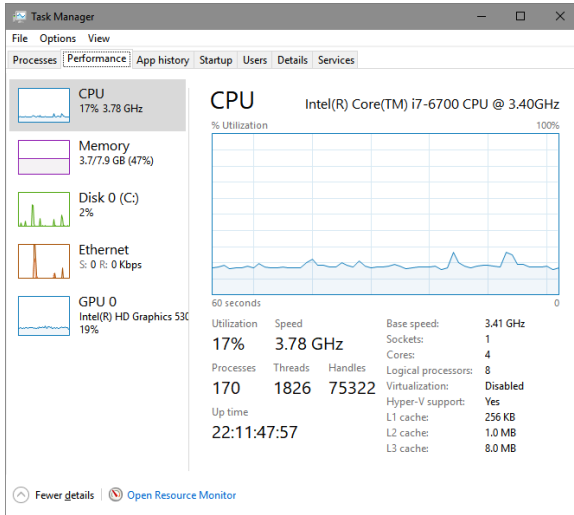


Figure II.5 ~ Computer system

Right: Lenovo M910 Small Form Factor (SFF) ThinkCentre PC equipped with Intel Core i7-6700, 3.4 GHz, 4-core processor and Windows 10 Pro x64. Image source: Lenovo

Left: The Windows Task Manager shows CPU usage performance (17%) while running SDRuno, two instances of Callisto software and a few other utilities including a UPS monitor. The memory usage is about 1.7 GB of 7.9 GB available. Memory was later increased to 24 GB.

II.3. Low Frequency Transmitter Stations

Thirteen low frequency transmitter stations were received with significant strength at Coho Radio Observatory during initial tests between June and September 2018 (table II.1). Of these, two disappeared during the measurement period, station TBB in Turkey on 26.7 kHz and a station with unknown call sign in Israel on 29.7 kHz. For TBB I recorded only the background noise for a couple days and made no measurements of the Israeli station. Also, the two Russian stations, at 18.1 and 21.1 kHz are both designated RDL, operate intermittently and were not recorded. I left these four stations on the list as a reminder for future studies.

The ideal radiation pattern for a small loop antenna is a figure-8 with maximum responses in the plane of the loop and minimum responses (nulls) perpendicular to the plane. All the transmitter stations for which data were taken are conveniently located either north-south or east-west of CRO. Since a loop antenna inherently has 180° directional ambiguity, it was possible to use only two antenna orientations to cover all the stations, 000°-180° (N-S) and 095°-275° (nominal E-W) (figure II.6).

Table II.1 ~Transmitter stations received at Cohoe Radio Observatory (see text)

Station	Location	Frequency (kHz)	Distance (km)	Direction (° TN)	Antenna Azimuth	Remarks
JXN	Gildeskål Norway	16.4	5773	007	N-S	Polar
RDL	Russia	18.1				No data
NWC	North West Cape Australia	19.8	12386	263	E-W	Near antipodal
RDL	Russia	21.1				No data
NPM	Hawaii USA	21.4	4390	190	N-S	
JJI	Miyazaki Japan	22.2	6297	277	E-W	
DHO38	Saterland Germany	23.4	7224	014	N-S	Polar
NAA	Maine USA	24.0	5464	068	E-W	
NLK	Washington USA	24.8	2272	113	E-W	
NML	North Dakota USA	25.2	3661	090	E-W	
TBB	Denizköy-Bafa Turkey	26.7	8756	360	N-S	Polar, noise
Unknown	Negev Desert Israel	29.7	9727	355	N-S	Polar, no data
NRK	Grindavik Iceland	37.5	3356	027	N-S	Polar

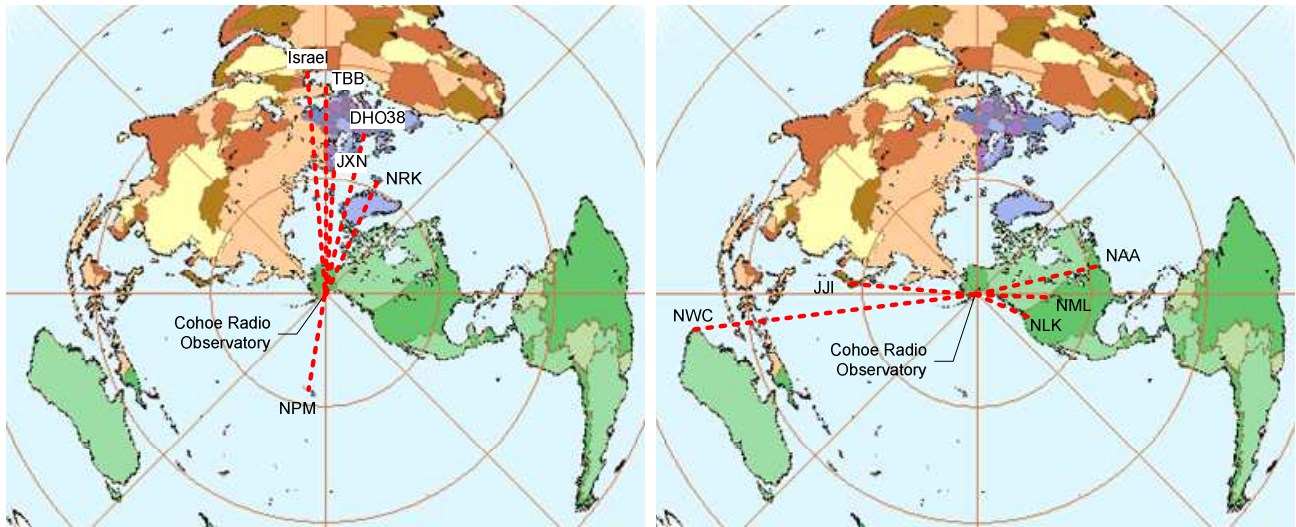


Figure II.6.a ~ World maps centered on Cohoe Radio Observatory with CRO north at top. The dashed red lines point to transmitter station locations. Of all the stations shown, NPM in Hawaii was by far the strongest. **Left:** Four of six stations were recorded with the antenna oriented N-S. Signals from stations TBB in Turkey and the unknown station in Israel were not recorded; **Right:** Five stations recorded with the antenna oriented E-W. Underlying map image source: F6DQM azimuthal map software ([AziWorld](#))

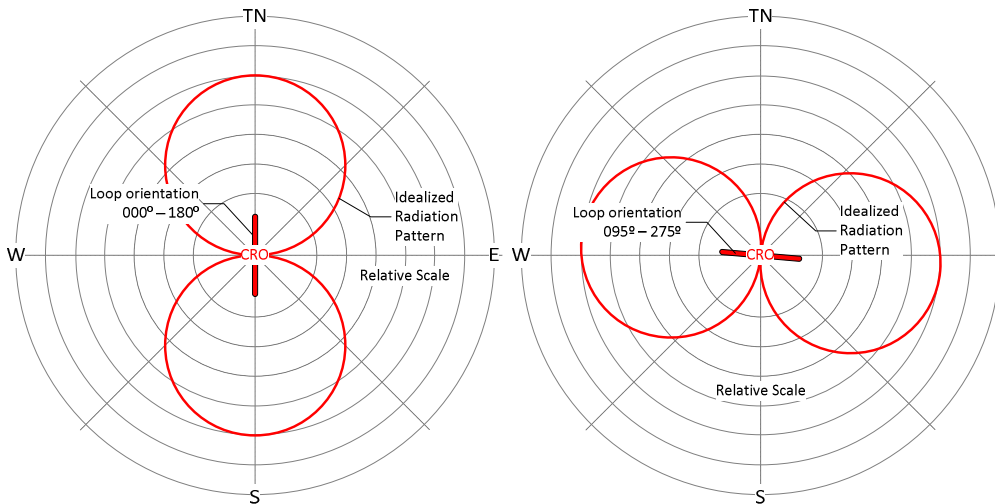


Figure II.6.b ~ Idealized radiation patterns for the loop antenna at Cohoe Radio Observatory. Left: Orientation for stations located approximately north and south of Cohoe; Right: Orientation for transmitter stations located approximately east and west of Cohoe. Images © 2018 W. Reeve

All information regarding transmitter station name, location, direction and distance given here is based on online data including {ReeveVLF}, {VLFList-1}, {VLFList-2}, {VLFList-3} and {VLFList-4}. It is noted that all these references are cross-dependent, may not be up-to-date and may include errors. Conventional demodulation of the signals yields no identity information. I could only verify a station by rotating the loop, noting the null direction and comparing it to the published location data. I also rotated the loop for maximum received signal and compared the directions, but the maximum is much broader than the null and only usable as a double-check.

II.4. Signal Measurements

The measurement schedule was based on grouping most stations according to direction (table II.2). Except as shown, I rotated the antenna to point east-west and then recorded the received signal level and signal-to-noise ratio (SNR) from the five stations to the east and west of Cohoe, each for 72 h. I then rotated the antenna to point north-south and recorded the signal level and SNR from the four stations to the north and south, again for 72 h each. I also recorded only the background noise at the frequency for one of the stations as previously mentioned. I recorded the strongest station, NPM on 21.4 kHz, at the beginning and end of the study period. The recorded stations were not the only stations received at CRO but they were the strongest and most consistent during the measurement period. Another 6 to 8 considerably weaker stations appeared between 10 and 40 kHz depending on time of day, and these may be studied in the future.

The initial receiver setup and antenna rotation was performed on-site at CRO. All other operations were performed remotely from Anchorage using TeamViewer software. It was only necessary to remotely adjust the receiver frequency and filenames associated with each recording session. Upon completion of a measurement run, I used the TeamViewer file transfer function to move the data files to Anchorage for processing. I had not yet installed remote control on the loop antenna rotator so changing the loop orientation from E-W to N-S required a site visit. The data gathering portion of this study required about 5 weeks, from 16 September through 19 October 2018. The time period was near the autumnal equinox, which provided an almost equal split of day and night during each 24 h period.

Table II.2 ~ Measurement schedule

Station	Start Date, Time (UTC)	End Date, Time (UTC)	Antenna
NPM, 21.4 kHz	16 September, 0405	19 September, 0414	N-S
JJI, 22.2 kHz	21 September, 1735	24 September, 1822	E-W
NML, 25.2 kHz	24 September, 1835	27 September, 1955	E-W
NLK, 24.8 kHz	27 September, 1959	30 September, 2007	E-W
NAA, 24.0 kHz	30 September, 2017	03 October, 2343	E-W
NWC, 19.8 kHz	03 October, 2350	07 October, 0001	E-W
JXN, 16.4 kHz	07 October, 0034	11 October, 0035	N-S
TBB, 26.7 kHz	11 October, 0038	13 October, 0337	N-S
NRK, 37.5 kHz	13 October, 0518	16 October, 0533	N-S
DHO38, 23.4 kHz	16 October, 0539	19 October, 1441	N-S

I used the *PWR & SNR TO CSV* function in SDRuno to sample and record the received signal power levels (PWR) and signal-to-noise ratios (SNR) at 30 s intervals for each of the stations previously listed. A local oscillator (LO) frequency of 91.099 kHz was used for all measurements. I chose the LO frequency to be above the maximum measurement frequency (40 kHz) but otherwise it was arbitrary; future measurements will use an LO frequency of 125.000 kHz. Gain was set to 36.1 in the SDRuno Main window (figure II.7). I used CW demodulation with 250 Hz bandwidth, wideband noise blanker (NBW) and turned the AGC Off but used no other special software settings in either the RX Control or EX Control windows (figure II.8). The AGC and demodulation mode affects only the demodulated signal fed to the PC sound system but have no effect on the displayed spectrum or data recordings. To smooth the spectrum displays I used FFT averaging, generally 4096 (2^{12}).



Figure II.7 ~ SDRuno Main window shows general and common receiver settings including antenna port, RF gain, sampling rate and decimation. Also, the receiver is started and stopped and virtual receivers are assigned from this window. Only one virtual receiver was used during this propagation study. The two horizontal meters at bottom-left indicate the PC system and software loads. In this case, the SDRuno software added 1% to the overall system load of 4%.



Figure II.8 ~ RX Control (left) and EX Control (right) windows for station NLK (24.8 kHz). These windows are used to control the settings for individual virtual receivers. Except for receiver frequency the same settings were used for all data recordings. The noise blanker (NB) threshold setting of 128 in the EX Control was determined experimentally as a compromise between loss of sensitivity and noise spike reduction.

The SDRuno software is capable of numerous virtual receivers, each setup on a different frequency within the spectral bandwidth being monitored. I potentially could have recorded the PWR and SNR levels simultaneously for all stations in this study. However, I found from previous experience that management of many virtual receivers and their associated windows is not as simple as it sounds. I also had an unanswered question about CPU resource requirements when trying to simultaneously record the data from four or five stations. For these reasons I chose to record data for only one station at a time.

II.5. Spectrum Analyses

I took occasional screenshots of the main spectrum (SP1) and IF spectrum (SP2) windows for later viewing and analysis. Several of the received signals were relatively quite strong and other weaker signals appeared throughout the day (figure II.9). The spectrum images contain a lot of useful information in addition to the signals; additional information on SDRuno operation and spectrum displays may be found in [Reeve18-1](#).

The signals can be examined in more detail in the IF spectrum window SP2 (figure II.10). The receiver IF spectrum is offset because I operated the receiver in *Zero-IF* mode with CW demodulation. The CW is offset (equivalent to a *beat frequency oscillator* or BFO used in an analog receiver) and set to 700 Hz. CW transmissions at, say, 24.8 kHz will be processed in the receiver IF and displayed as 700 Hz tones in the SP2 window. Note that the AM and SSB modes display the same signals without any offset. As expected, the main spectrum display, SP1, varies not only throughout the day and over longer time periods but also with antenna azimuth (figure II.11).

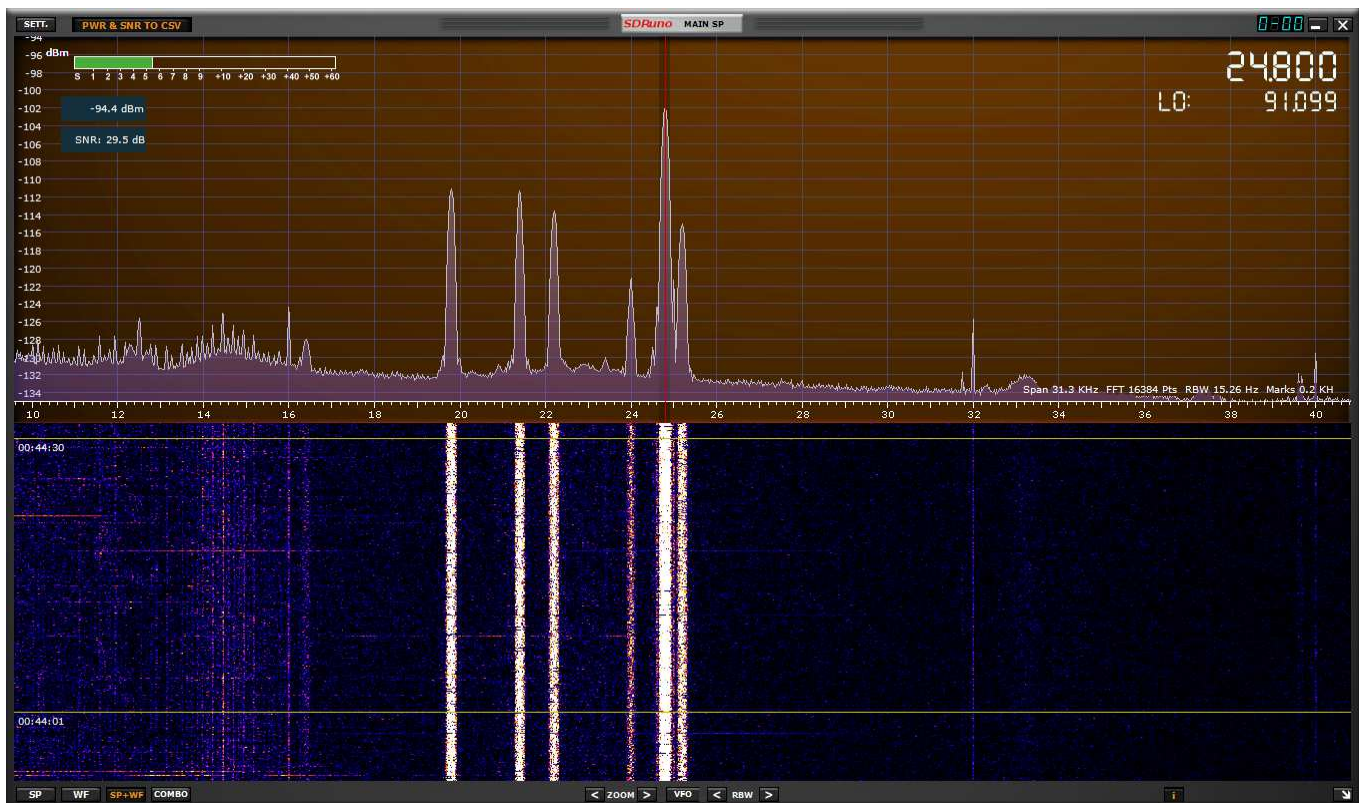


Figure II.9.a ~ Main Spectrum SP1 window shows received spectrum and waterfall at 0044 UTC on 30 September (1644 on 29 September local time) about 3 h before local sunset. The antenna is oriented east-west and favors stations in those directions. The spectrum is setup to display a frequency range from about 10 to 40 kHz with tick marks at 200 Hz intervals. The displayed resolution bandwidth is about 15 Hz – see text just above the frequency scale on the right of the spectrum for this and other parameters. In this image the receiver is tuned to station NLK at 24.8 kHz, which is indicated by a red vertical cursor in the spectrum at that frequency. The other signals seen in the main spectrum are VLF transmitters at 16.4, 19.8, 21.4, 22.2, 24.0, 25.2 and possibly 33.3 kHz. The signal at 24.8 kHz is the strongest and its 1.2 MW transmitter is in Washington USA only a couple thousand kilometers away from Cohoe. Received signal power levels in dBm and SNR in dB are displayed on the upper-left of the spectrum window. The SNR is based on the noise in the IF spectrum.

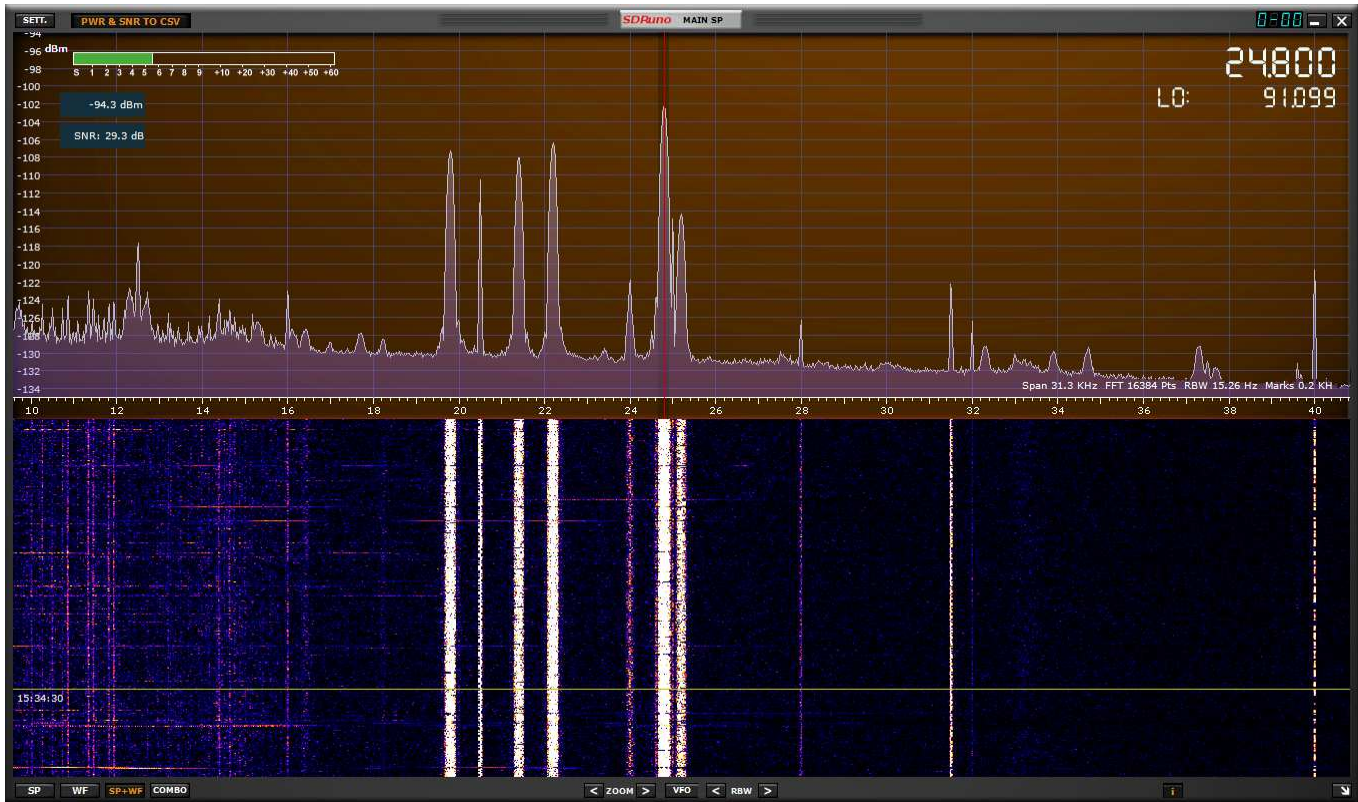


Figure II.9.b ~ Received spectrum and waterfall window about 15 h later than previous image but with same settings. This image was taken at 1530 UTC on 30 September (0730 local time on 30 September, about 40 min before local sunrise). In addition to the strong signals already noted in the previous figure, signals appear in this spectrum display at 16.2, 17.7, 18.2, 20.5, 31.5, 32.3, 32.9, 33.9, 37.3, 37.5 and 37.7 kHz. Most of these are relatively weak and a few may be spurious, but they are persistent enough to be carried through the FFT averaging process (FFT averaging is purely a visual process in SDRUno).

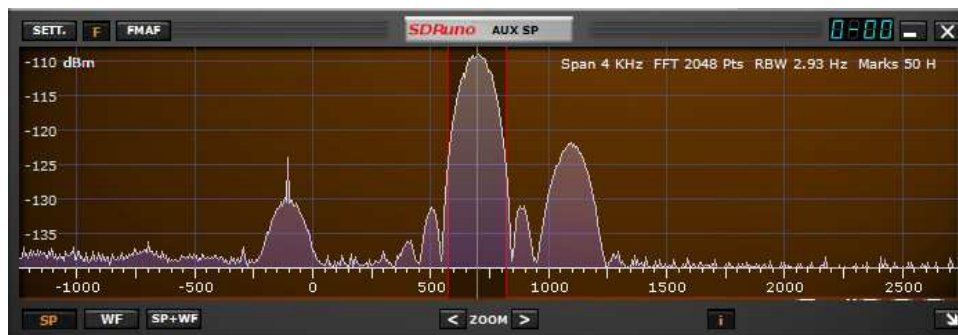


Figure II.10 ~ Auxiliary Spectrum SP2 window shows the IF spectrum, in this case an IF range of -1000 to +2500 Hz with tick marks at 50 Hz intervals. The resolution bandwidth is about 3 Hz. The receiver signal at 24.8 kHz is bracketed by red cursors centered on the zero IF frequency but offset by 700 Hz. The cursors indicate the edges of the demodulation filter (250 Hz CW filter) and are located at 700 ± 125 Hz. Note the two sidebands at +500 and +900 Hz (± 200 Hz from the center frequency). Another signal is visible at +400 Hz but it could be spurious or a weak station at 24.5 kHz. Additional signals are seen at -100 and +1100 Hz, corresponding to the stations at 24.0 and 25.2 kHz. A receiver spur or birdie is visible at -100 Hz, superposed on the received signal at 24.0 kHz. The RSP2Pro shows such spurious spikes at 8 kHz intervals when the receiver is set for low frequencies.

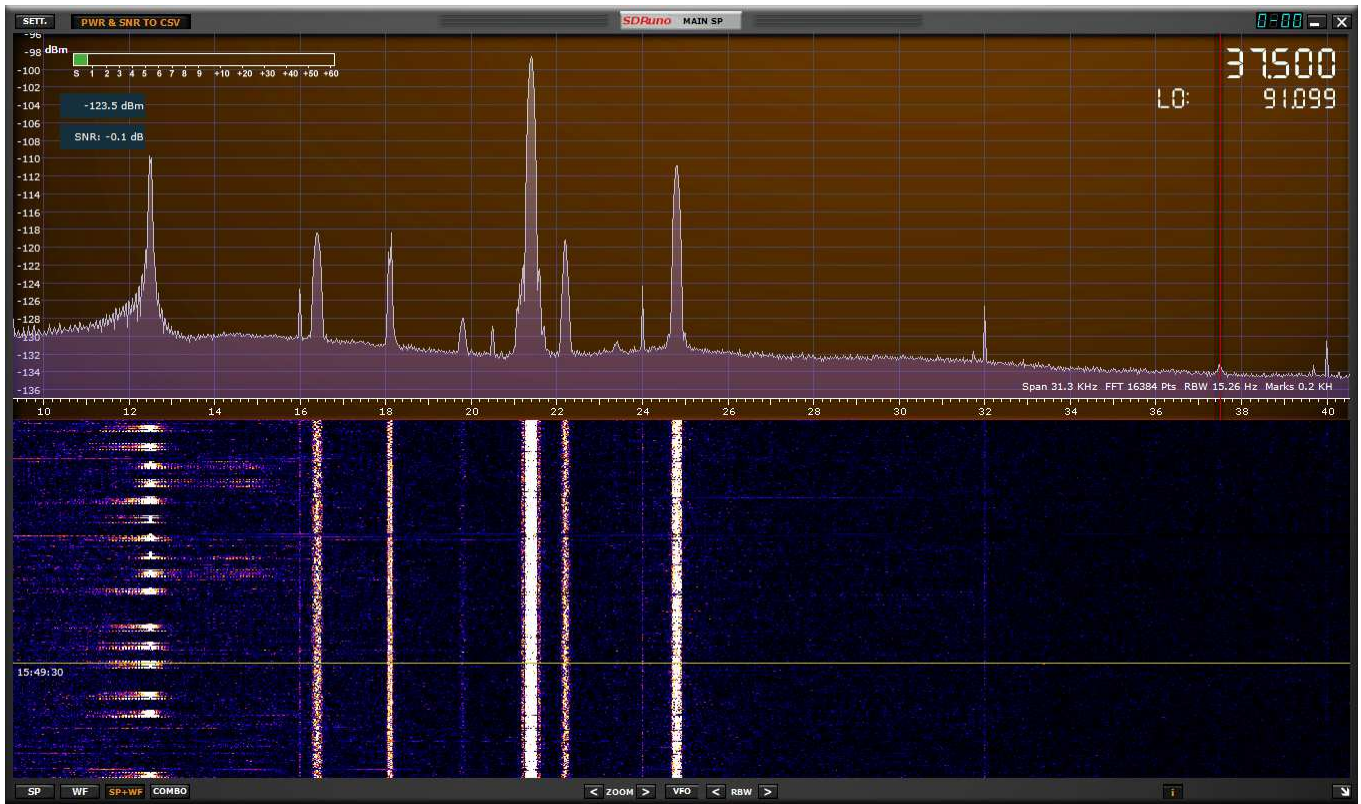


Figure II.11.a ~ Received spectrum and waterfall window for 15 October at 1550 UTC (0750 local time). The window is setup as shown previously except the receiver being recorded is on 37.5 kHz (station NRK in Iceland), which is very weak. The strongest station is NPM in Hawaii at 21.4 kHz and it may be hiding a station at 21.2 kHz. Other signals appear at 16.4, 18.1, 19.8, 20.5, 22.2 and 24.8 kHz. A few spurious signals also are present including a strong recurring impulse at 12.5 kHz.

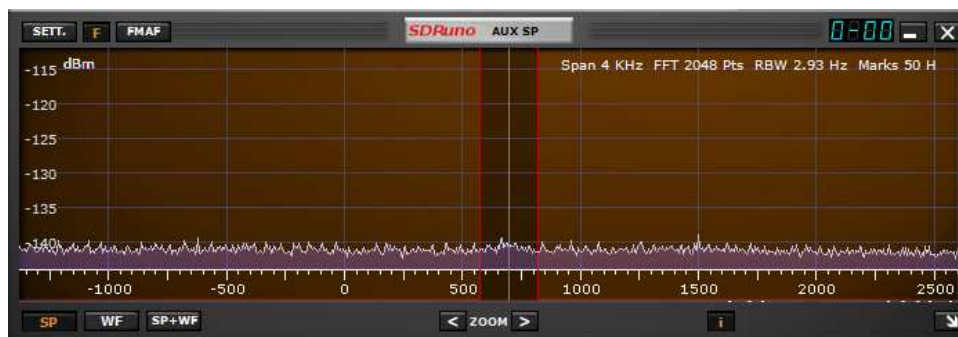


Figure II.11.b ~ Auxiliary Spectrum SP2 window image for the station at 37.5 kHz taken at the same time as the previous main spectrum image. The received signal is so weak it is not visible against the background noise.

II.6. Received Power and Signal-to-Noise Ratio

The *PWR & SNR TO CSV* function in SDRuno saves the data along with date and time stamps as Comma Separated Variable (.csv) files (figure II.12). One file covering a 72 h period was produced for each station. Each saved CSV file was about 350 kB (equivalent to about 4.9 kB h⁻¹) and consisted of around 8640 data points. The files were opened later in the Excel spreadsheet program and the data columns plotted as X-Y charts (figure II.13). The default displayed format for the date and time stamp data column in the CSV file is m/d/yyyy hh.mm but the data include seconds. To confirm the sampling interval the column can be reformatted as m/d/yyyy hh.mm.ss to reveal the seconds. In all the plots shown in this section, the power level data on the plots are associated with the primary vertical scale (left) and the SNR data are associated with the secondary vertical scale (right). All station plots use the same vertical scales for direct comparison.

Date Stamp	VFO Freq (Hz)	Power (dBm)	SNR (dB)
9/27/2018 19:59	24800	-122.4	0.7
9/27/2018 20:00	24800	-121.2	1.2
9/27/2018 20:00	24800	-122	0.6
9/27/2018 20:01	24800	-122.6	5.4
9/27/2018 20:01	24800	-121.6	2.1
9/27/2018 20:02	24800	-117.2	1.8
9/27/2018 20:02	24800	-123.5	3.2

Figure II.12 ~ Example shows the first eight rows of the PWR & SNR file for the 24.8 kHz receiver settings. Four columns of data are saved. The default format for the Date Stamp column does not show seconds. The frequency is captured in a column in case it is changed while the data are collected.

My main interest in the SNR plots was to see if they contained useful information not already available in the PWR plots. The SNR follows the PWR except that the SNR shows numerous short and deep decreases. This probably was due to impulse noise bursts momentarily lowering the SNR but not affecting the PWR. In any case, the SNR data appears to be redundant and provides no additional information for my purposes. Although SNR always is included in the saved data, it does not have to be plotted.

The signal level plots for the weaker stations are full of impulse noise that would make SID detection difficult or impossible. The thresholds for smooth plots appear to be a nighttime received power level around -90 dBm and a daytime level around -95 dBm. The indicated signal power levels are factory calibrated and are referenced to the receiver RF input connector. Indications of -90 and -95 dBm for night and day appear to be sufficiently above the local impulse noise floor, at least for the receiver settings and antenna configuration in this group of measurements. Note that the difference between night and day signal levels is 5 dB. Examination of the plots indicates that impulse noise levels appear to be slightly higher in the north-south than east-west directions. The north-south direction encompasses more people and industrial facilities on the Kenai Peninsula including the CRO observatory building itself.

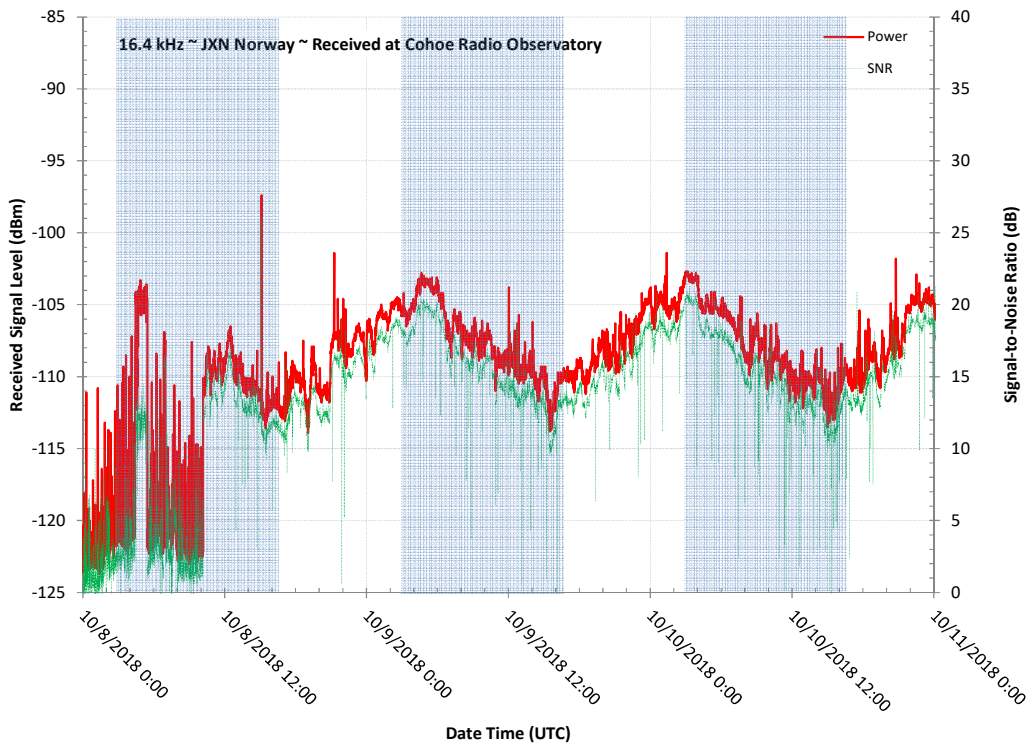


Figure II.13.a ~ Received PWR and SNR for station JXN in Norway. Off the air during the first two days measurement period starting 6 October, so it was extended an extra day to 10 October. The plot initially indicates the no-signal noise level at 16.4 kHz. The signal returns for about 1 h at about 0300 UTC on 8 October and then returns continuously at 1000. The signal is not badly corrupted by impulse noise but is weak and does not provide a clear indication of sunrise or sunset.

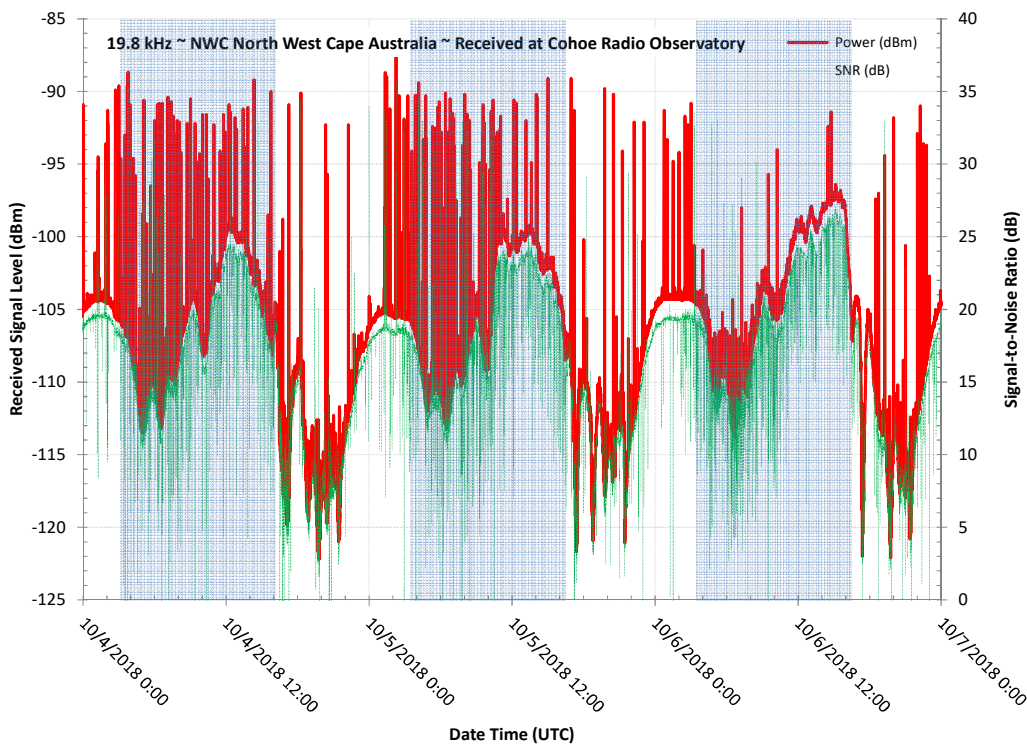


Figure II.13.b ~ Received PWR and SNR for station NWC at North West Cape in Australia. The propagation throughout any given day and night is quite complicated as indicated by the multiple periodic increases and decreases in received signal level. Some of this is likely due to interference patterns produced as the ionosphere height changes along the path. The impulse noise appears to be greatest during the local nighttime but tapers off on the third day.

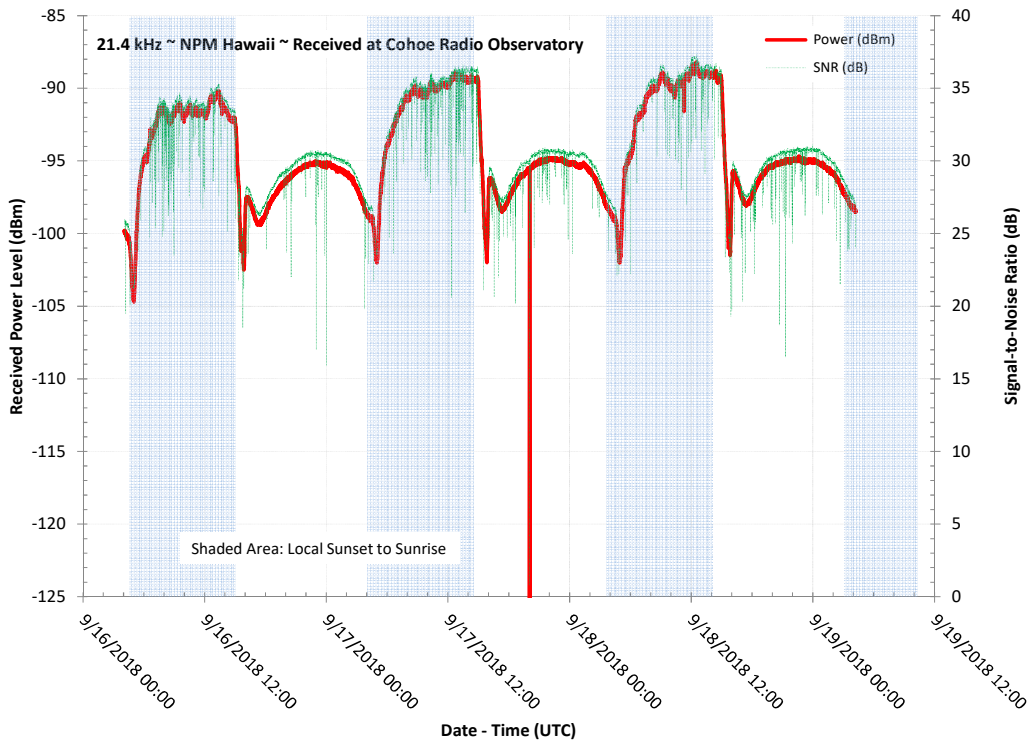


Figure II.13.c ~ Received PWR and SNR for station NPM in Hawaii USA. The strong signal provided a smooth plot.

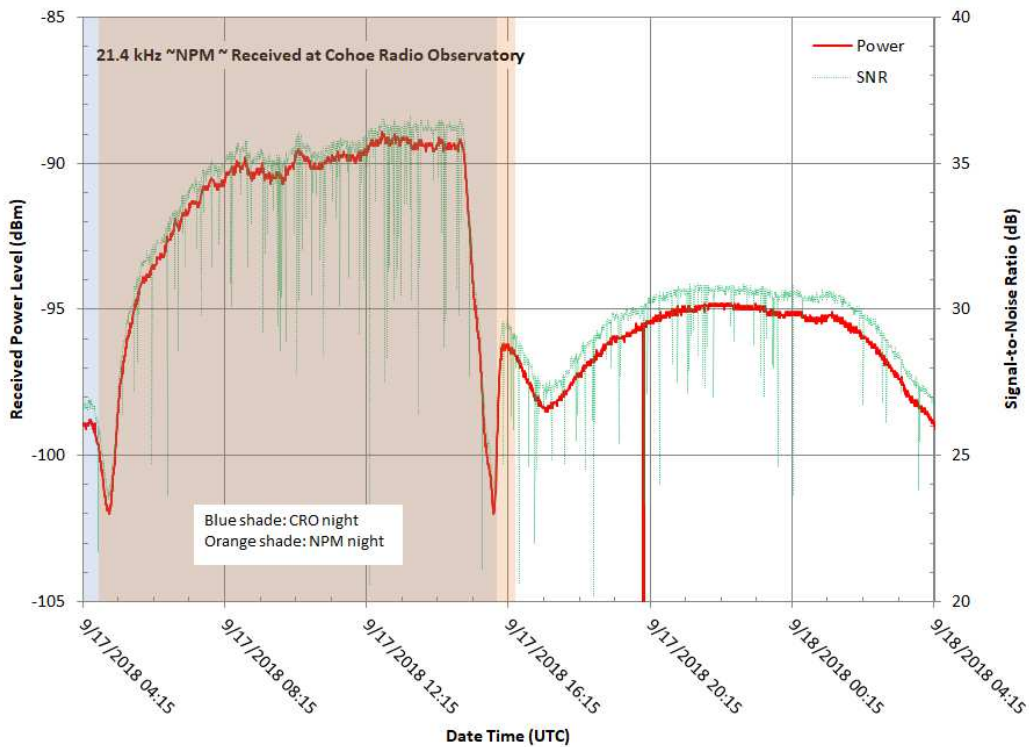


Figure II.13.d ~ Part of above plot for station NPM covering the 24 h period from 0415 UTC on 17 September to 0415 on 18 September. The sunset and sunrise signatures – a dip in the received signal level – are clearly seen. There is a short transmitter dropout at 2000 on 17 September.

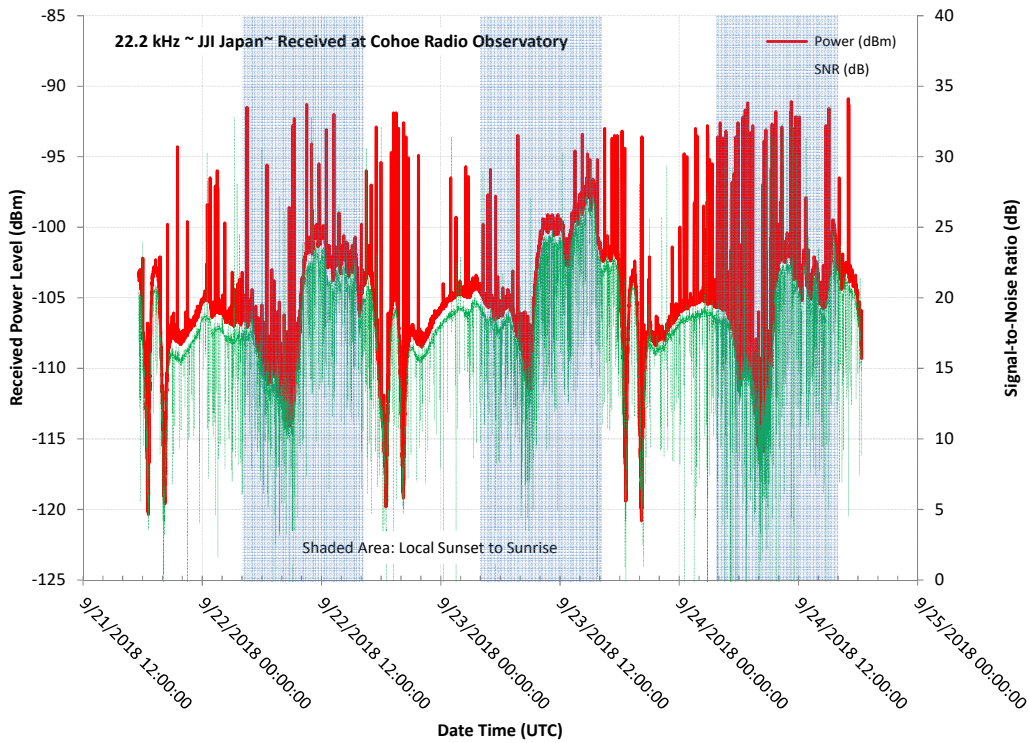


Figure II.13.e ~ Received PWR and SNR for station JJI in Japan. Note the almost complete signal drop-outs at approximately 2 and 4 h after each local sunrise.

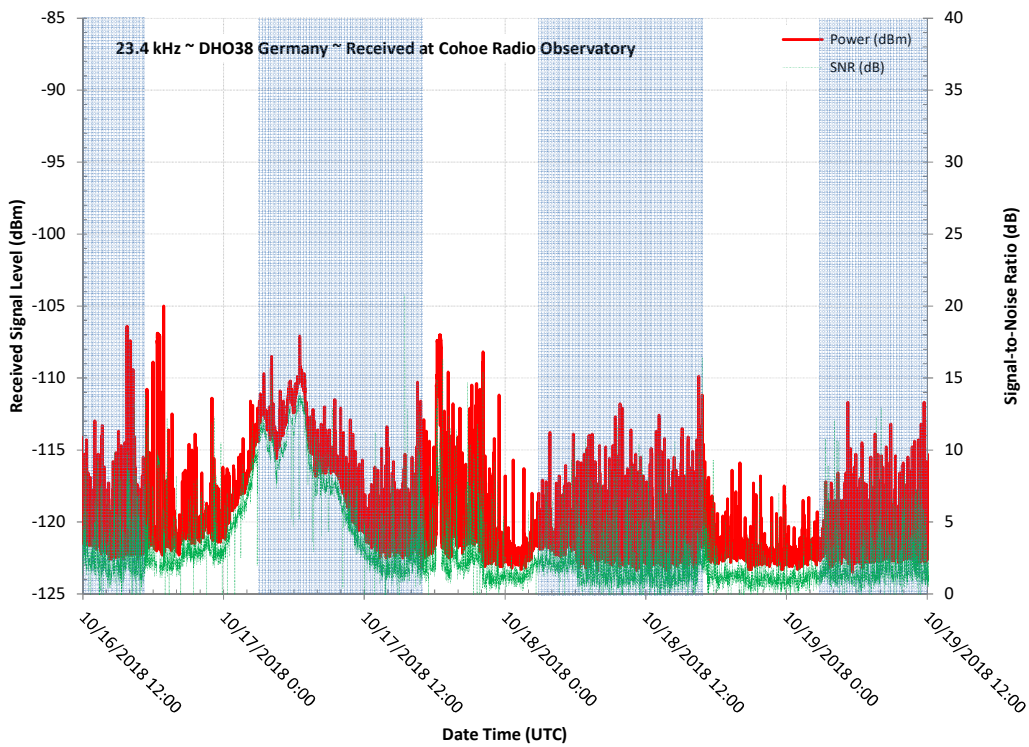


Figure II.13.f ~ Received PWR and SNR for station DHO38 Germany. Polar path. Weak signal apparently with outages except on first day. Precipitation is a possible cause for the high noise levels.

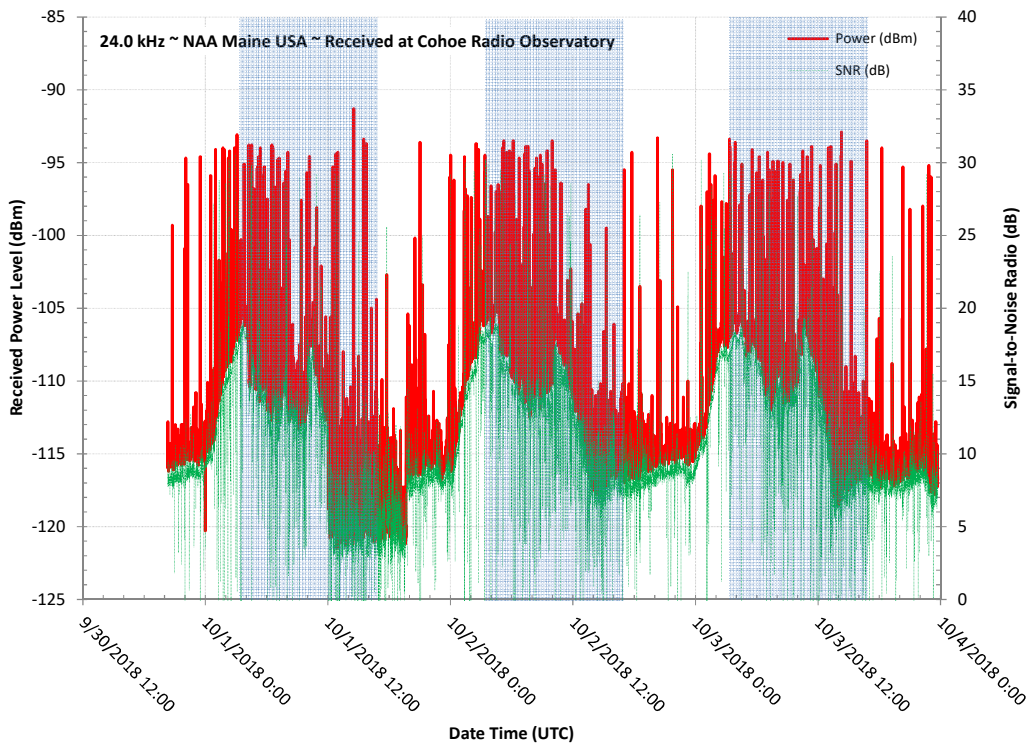


Figure II.13.g ~ Received PWR and SNR for station NAA in Maine USA. Signal dropout between 1200 and 1600 UTC on 1 October.

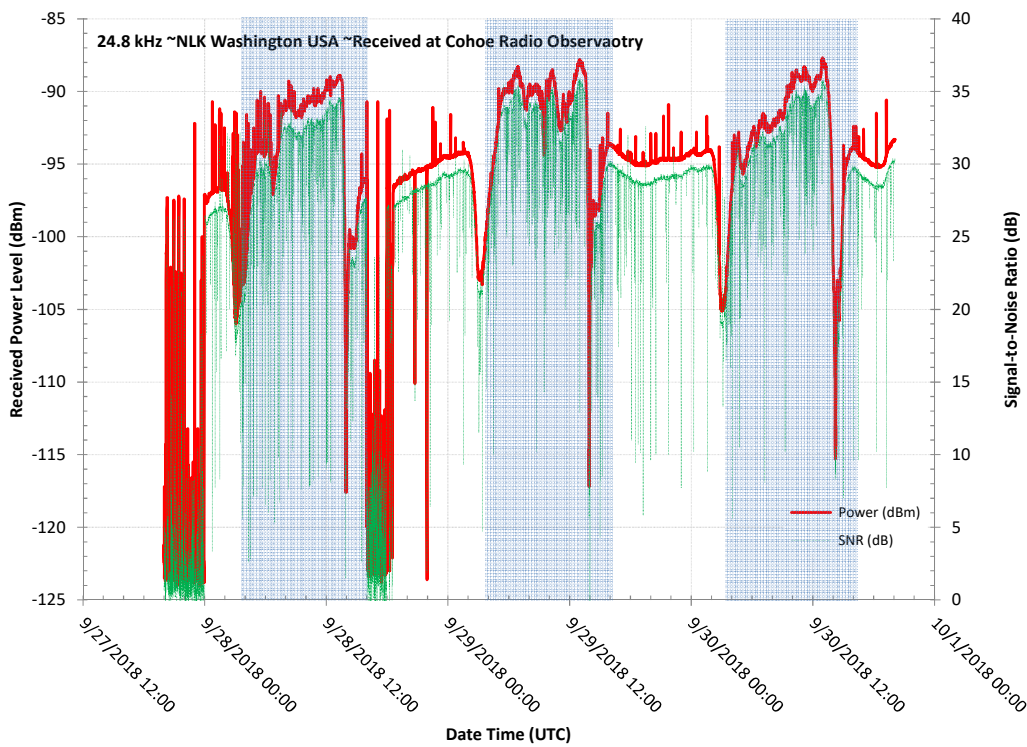


Figure II.13.h ~ Received PWR and SNR for station NLK in Washington USA. The signal dropout from 2200 to 2400 on 27 September and again from 1600 to 1800 on 28 September (sharp drop in PWR and SNR) probably is due to transmitter shutdown. The signal dips related to sunrises and sunsets are seen about 1 h before Cohoe and corresponds o the times at the transmitter site.

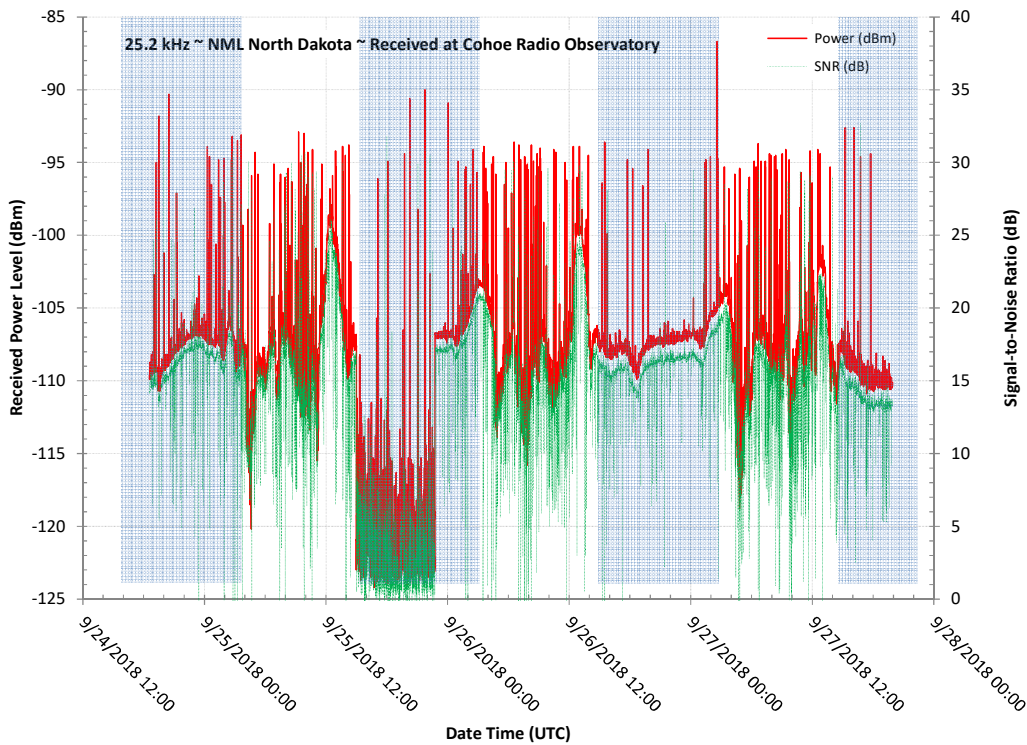


Figure II.13.i ~ Received PWR and SNR for station NML in North Dakota USA. Station off the air between about 1400 and 2300 on 25 September.

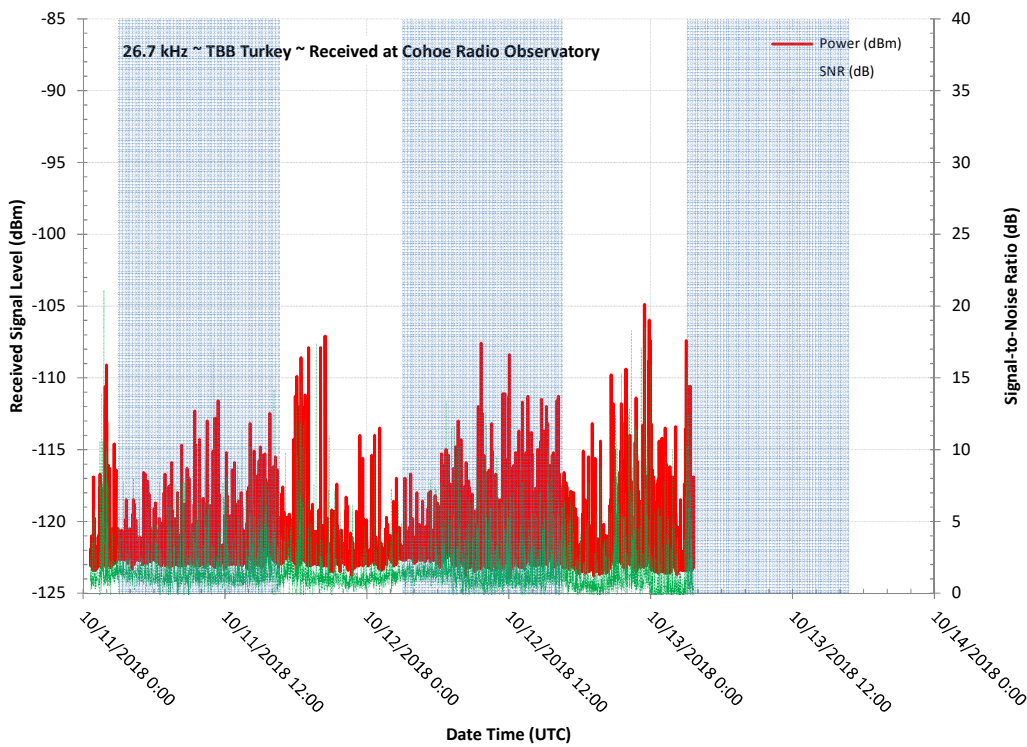


Figure II.13.j ~ Received PWR and SNR for station TBB in Turkey. This station was off the air during the measurement period from 11 through 14 October and only 2 days of background noise at 26.7 kHz were recorded. Note the 0 dB signal-to-noise ratio and the noise floor at about -123 dBm.

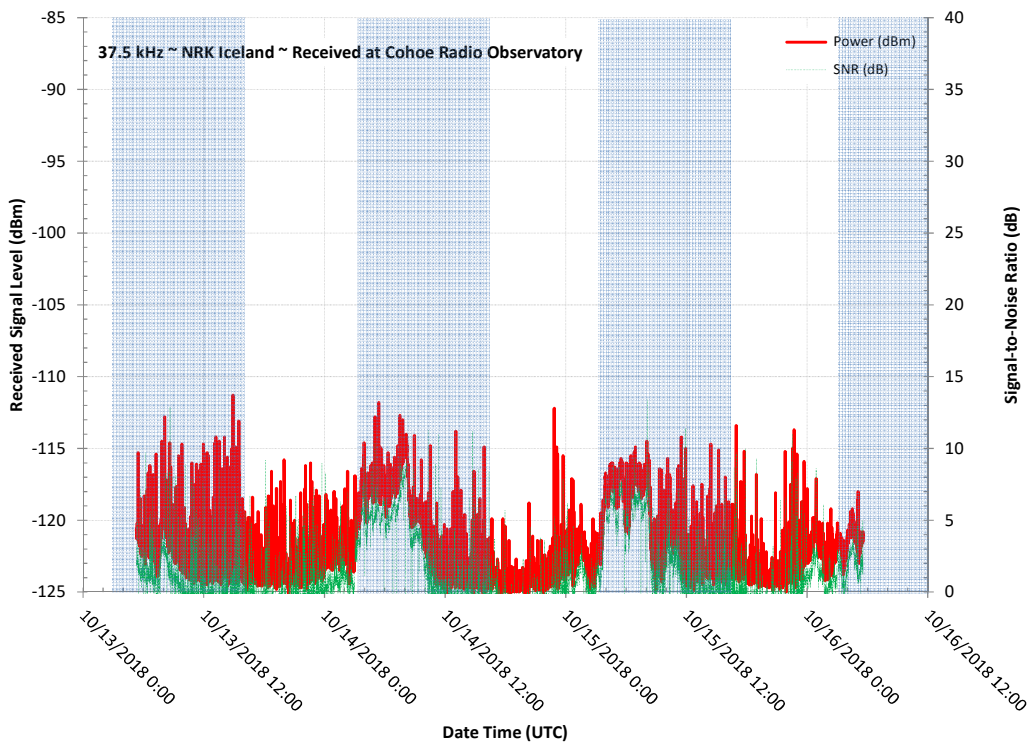


Figure II.13.k ~ Received PWR and SNR for station NRK in Iceland. The signal is easily discernible in spectrum displays but probably is too weak for SID detection.

II.7. Discussion

For my purposes, the SNR data provide no information not already provided by the PWR data, but it may be used to establish a minimum threshold for a smooth plot. For the receiver and antenna setup described here, the minimum daytime SNR for a smooth plot is about +30 dB (further investigation is required to determine if the threshold depends on direction). A loop antenna with more windings or larger physical area likely would improve the signal level plots for weaker stations. For the loop dimensions used here a different winding method would be necessary to reduce winding capacitance and keep the self-resonant frequency above about 40 kHz.

It is possible that changes in the receiver setup such as software settings or hardware configuration may reduce the effect of local impulse noise on the signal data and plots. It is noted that the newer SDRPlay RSPduo is supposed to have better low frequency performance than the RSP2Pro used here, and I plan to make future measurements with the newer receiver. However, better sensitivity in the face of the same external impulse noise may not provide any overall improvement.

Another possibility for reducing the effects of impulse noise is to lowpass filter the RF signal before it enters the receiver. This would require a special filter design because of the balanced transmission line, impedances and low frequencies involved. It may be possible to post-process the data to reduce the impulse noise by removing signal samples that exceed a certain threshold or by data averaging. A simple running average or smoothing function, both of which are lowpass filter processes, may prove useful.

The background noise level viewed on the spectrum plot is highest at the low frequency limit of the observations and steadily tapers lower toward the high frequency limit. This variation may be due to the antenna or receiver response. The noise displayed on the spectrum plots has been averaged and is lower than the instantaneous noise. On the basis of the received power plots for each station, which are not averaged, the noise floor is about -123 dBm and is the same for north-south and east-west antenna azimuths. One station (NAA at 24.0 kHz) shows a noise floor about -120 dBm but this is an exception.

A considerable amount of rain fell on Cohoe during the study period especially in early October (figure II.14), and this may have affected the loop antenna characteristics because the windings are exposed to the weather. The dielectric constant of water is about 80 times that of dry air, so I would expect the rain to increase the distributed capacitance of the loop windings and lower the antenna's self-resonant frequency. Perhaps more importantly, static caused by the precipitation adds noise and this may reduce the signal-to-noise ratios of the stations recorded during rain. Examination of the plots indicates the noise floor is relatively constant at -123 dBm during the drier periods but increases by 1 or 2 dB during the rainy periods in early October.

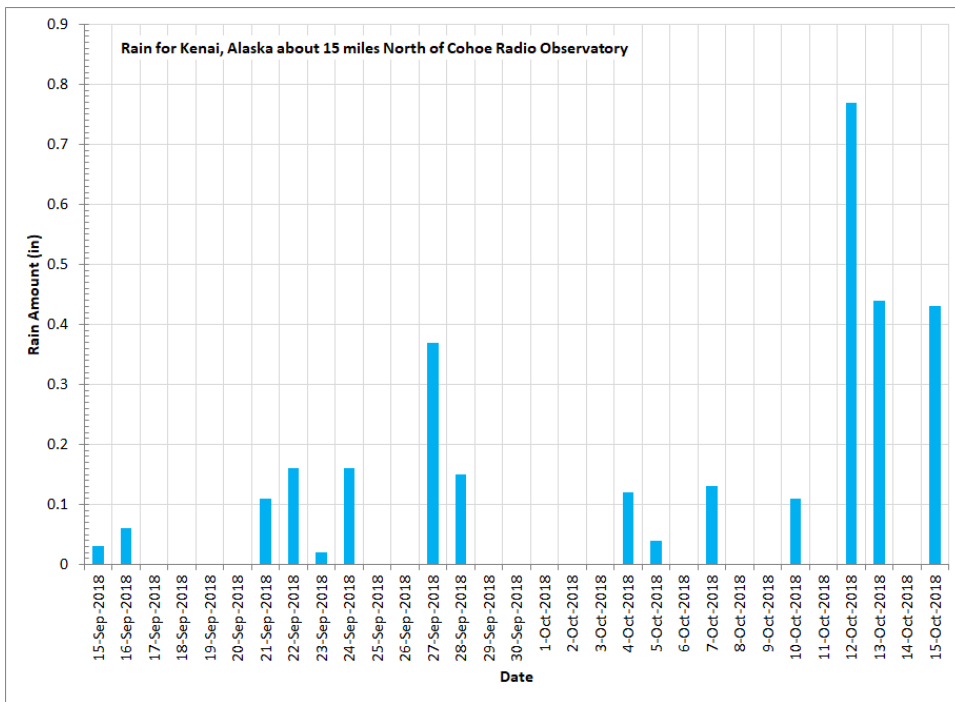


Figure II.14 ~ Rain during study period for Kenai, Alaska, about 15 mi (24 km) north of CRO. Data source: NOAA, National Center for Environmental Information

Being able to control the SDR receiver using a remote desktop program like TeamViewer significantly simplified data collection. Not being able to control the antenna rotation was a minor inconvenience for the measurements made during this study. The transmitter stations all were in fairly narrow azimuth ranges of either north-south or east-west, and this simplified antenna management. I regularly travel to Cohoe during summer and could rotate the antenna as needed while there. Nevertheless, remote rotation control would improve overall flexibility in this installation especially during winter when travel is less frequent.

Propagation paths that cross the North or South Pole from a low frequency transmitter to a receiver – polar paths – are not unique to CRO. However, CRO is located just south of the auroral oval and the Earth's magnetic

field has an inclination of 73°. The magnetic field has a strong influence on radio propagation in the Earth-ionosphere waveguide and study over a longer time period may yield interesting results.

The measurements for each station spanned only three days during fall 2018. It would be interesting to make longer term measurements spanning, say, one year during the current low in the solar cycle. Even longer study periods would span a complete solar cycle, requiring a dedication to purpose that would be hard to sustain for a private observatory (that is, an observatory that has no government funding).

II.8. References and Weblinks for Part II

- [ReeveP1] Reeve, W., Monitoring Low Frequency Propagation with a Software Defined Radio Receiver, Part II ~ Observations, 2018
- {Reeve18-1} Reeve, W., Initial Results from VLF and LF Observations at Coho Radio Observatory, 2018, available at: http://www.reeve.com/Documents/Articles%20Papers/Reeve_CohoVLFInitial.pdf
- {Reeve18-2} Reeve, W., Reception of SAQ Transmissions at Coho Radio Observatory on 1 July 2018, 2018, available at: http://www.reeve.com/Documents/Articles%20Papers/Reeve_SAQ-Jul2018.pdf
- {Reeve18-3} Reeve, W., Square Loop Antenna, 1.2 m Diagonal ~ Mechanical and Electrical Characteristics and Construction Details, 2018, available at: http://www.reeve.com/Documents/Articles%20Papers/Reeve_SquareLoopAntenna1.2m.pdf
- {AziWorld} <http://f6dqm.free.fr/soft/aziworld/en/aziworld.htm>
- {ReeveVLF} http://www.reeve.com/Documents/Articles%20Papers/Reeve_VLF-LFStationList.pdf
- {VLFList-1} <https://www.mwlist.org/vlf.php>
- {VLFList-2} <https://sidstation.loudet.org/stations-list-en.xhtml>
- {VLFList-3} <https://www.smeter.net/stations/vlf-stations.php>
- {VLFList-4} <http://www.vlf.it/trond2/list.html>



Author - Whitham Reeve is a contributing editor for the SARA journal, Radio Astronomy. He obtained B.S. and M.S. degrees in Electrical Engineering at University of Alaska Fairbanks, USA. He worked as a professional engineer and engineering firm owner/operator in the airline and telecommunications industries for more than 40 years and now manufactures electronic equipment used in radio astronomy. He has lived in Anchorage, Alaska his entire life. Email contact: whitreeve@gmail.com

Document Information

Author: Whitham D. Reeve

Copyright: ©2019 W. Reeve

Revisions: 0.0 (Original draft pulled from Cohoe VLF paper, 21 Aug 2018)
0.1 (Added location details and maps, 29 Sep 2018)
0.2 (Added 1st group of PWR and SNR plots, 01 October 2018)
0.3 (Numerous minor edits, added NWC plot, 07 Oct 2018)
0.4 (Added last group of plots, 19 Oct 2018)
0.5 (Added receiver and PC images and updated all plots, 03 Nov 2018)
0.6 (Preparation for distribution, 23 Jan 2019)
0.7 (Minor edits prior to distribution, 25 Jan 2019)
0.8 (Minor edits for distribution, 20 Feb 2019)

Word count: 4759

File size (bytes): 63060992